THE WAKE STRUCTURE FROM FRACTAL FENCES: IMPLICATIONS FOR THE CONTROL OF TURBULENT SUSPENSIONS

Keylock C.J.[1], Nishimura K.[2], Nemoto M.[3], Ito Y.[2]

[1] Earth and Biosphere Institute and School of Geography, University of Leeds, UK

[2] Nagaoka Institute for Snow and Ice Studies, Suyoshi, Nagaoka, Niigata, 940-0821, Japan.

[3] Nagaoka Institute for Snow and Ice Studies – Shinjo Branch, 1400 Tokamachi, Shinjo, Yamagata, 996-0091, Japan.

In aeolian and snow-affected environments, deposition of saltating or suspended particles is often encouraged through the use of fences with a specific height and porosity. However, recent research in the fluid mechanics literature on fractal generated turbulence[1,2] implies that the fractal dimension of the object may also be an important control. In order to study this hypothesis we examined the deposition of snow particles and the turbulence structure (Fig. 1) behind fences of a fractal and non-fractal nature (Fig. 2) in the Shinjo Cryospheric Environmental Simulator wind tunnel (Fig. 3). The fences were chosen in such a way that the porosity and number of struts varied (Table 1). Here we report the longitudinal velocity measurements corrected for high turbulence conditions[3].

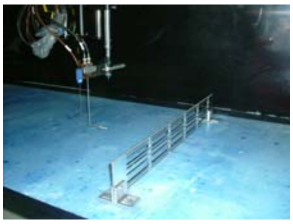

Figure 1. Hot wire anenometry measurements behind a fractal fence.

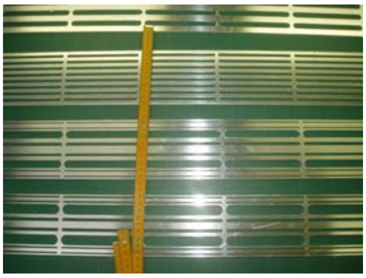

Figure 2. From top to bottom fences 5struts50, 9struts50, Frac50 and Frac60. Plate10 (a 90 mm solid plate with a 10 mm gap at the base) is not shown.

Figure 3. The 10m wind tunnel in the Shinjo Cryospheric Environmental Simulator.

Fence name	Porosity (%)	No. of horizontal struts	Mean (standard deviation) of strut spacing excluding the 10 mm bottom gap	Linear fractal dimension (D_f)
Plate10	10	1	0.00 (0.0) mm	1.000
5struts50	50	5	10.00 (0.0) mm	1.000
9struts50	50	9	5.00 (0.0) mm	1.000
Frac50	50	9	5.00 (4.4) mm	0.842
Frac60	60	9	6.25 (5.5) mm	0.774

Table 1. A description of the five fences used in this study..

Figure 4 shows that the turbulence levels are higher behind the fractal fences, but that these effects do not persist a significant distance downstream. However, when one examines the results in more detail, the difference in the wake characteristics are marked at distances of at least $x/H = 10$ (H is fence height). If the fence scale wave number is given by k^{*1} the wavenumber corresponding to the average forced scale is k^{*2} and the minimum forced scale (given by the narrowest strut) is $k^{*3,}$ then if $\varepsilon = 2\nu \int k^2 E(k)\,dk$, the fraction of dissipation occurring over the forced scales is

$$\varepsilon_{frac}(i,j) = \int_{k^{*i}}^{k^{*j}} k^2 E(k)\,dk \Big/ \int_0^{\infty} k^2 E(k)\,dk$$

The most important range for comparison is between k^{*1} and k^{*2} because the fractal objects inherently have a lower minimum forced scale but were designed to have a similar k^{*2} as 9struts50 (Table 1). Fig. 5 and 6 show that dissipation is higher for the fractal fences, providing the first experimental support for DNS results[2] of fractal-forced turbulence.

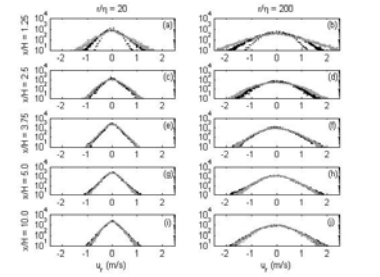

Figure 4. Longitudinal velocity increment distributions at $z / H = 0.55$ at various locations downstream of the fences and for two values of r / η. The grey dotted line is Frac60, the gray solid line Frac50, the black dotted line is 9struts50 and the solid black line is 5struts50.

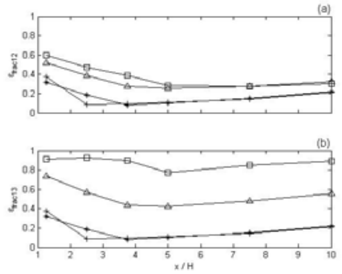

Figure 5. Values for $\varepsilon_{frac(1,2)}$ (a) and $\varepsilon_{frac(1,3)}$ (b) at height of $z / H = 0.55$ and varying x / H. Symbols correspond to: * (5struts50), + (9struts50), Δ (Frac50), □ (Frac60).

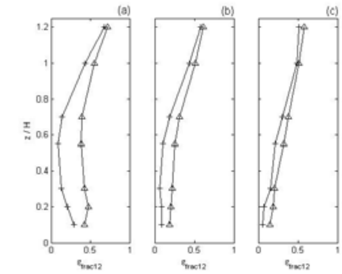

Figure 6. Values for $\varepsilon_{frac(1,2)}$ as a function of z / H at $x / H = 2.5$ (a), $x / H = 5.0$ (b) and $x / H = 10.0$ (c). Symbols correspond to: + (9struts50), Δ (Frac50).

In addition, if we estimate the third order structure function as[4] $\tilde{S}_3 = \left\langle \left| u(x+r) - u(x) \right|^3 \right\rangle$ and then use Extended Self-Similarity[5] to evaluate the exponent in $S_n(r) \sim r^{\zeta_n}$, denoting ESS-derived exponents as $\zeta_{n/3}$ and analysing the range from 20 r / η to 0.75 Λ, the fractal fences are clearly different to the non-fractal fences and yield exponents closer to those of K41 and She and Leveque[6] (Fig. 7-9).

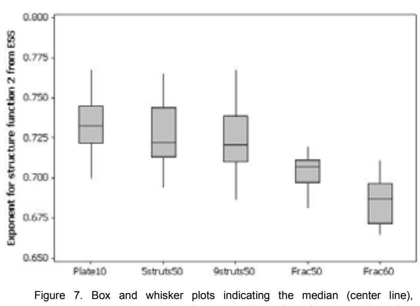

Figure 7. Box and whisker plots indicating the median (center line), interquartile range (box) and Q3 + 1.5 (Q3 - Q1), Q1 - 1.5 (Q3 - Q1) (whiskers) for the values of $\zeta_{2|3}$ determined over the sampled region.

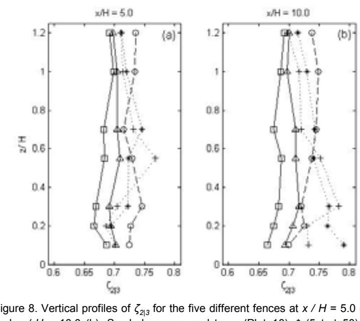

Figure 8. Vertical profiles of $\zeta_{2|3}$ for the five different fences at $x / H = 5.0$ (a) and $x / H = 10.0$ (b). Symbols correspond to: ○ (Plate10), * (5struts50), + (9struts50), Δ (Frac50), □ (Frac60).

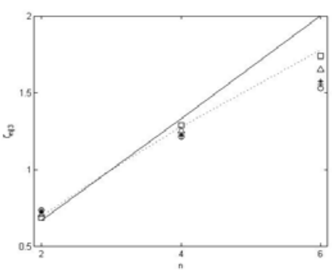

Figure 9. Mean values for $\zeta_{n|3}$ in the wakes for the five fences. The symbols used for each fence correspond to those in Fig. 8. The K41 theory is shown by a solid line and that due to She and Leveque [6] is indicated by a dotted line.

CONCLUSION: Even for much simpler objects than are typically studied[1,2], the fractal nature can have a significant effect on the turbulent wake structure, implying a need for revised design criteria for control structures. Our results also provide experimental evidence for phenomena detected in DNS studies.

REFERENCES:

[1] A. Staicu, B. Mazzi, J. C. Vassilicos, and W. van de Water, Phys. Rev. E **67**, 066306, (2003).
[2] B. Mazzi, and J. C. Vassilicos, J. Fluid Mech. **502**, 65, (2004).
[3] J.-F. Pinton, and R. Labbé, R., J. Phys. II **4**, 1461, (1994).
[4] S. G. Saddoughi, and S. V. Veeravali, J. Fluid Mech. **268**, 333, (1994).
[5] R. Benzi, S. Ciliberto, R. Tripiccione, C. Baudet, and S. Succi, Phys. Rev E **48**, 29 (1993).
[6] Z. S. She, E. Leveque, Phys. Rev. Lett. **72**, 336, (1994).

ACKNOWLEDGEMENTS:

This work was supported by JSPS short-term fellowship PE 04511 awarded to CJK.